FINAL REPORT

ERRORS INCURRED IN THE REDUCTION AND MATHEMATICAL MODELING OF PROCESS DYNAMIC DATA

A Research Project Supported by a NASA Grant
in the Space Related Sciences

NsG-518

Project No. DRI-612

June 1966

UNIVERSITY OF DENVER

FINAL REPORT

ERRORS INCURRED IN THE REDUCTION AND MATHEMATICAL MODELING OF PROCESS DYNAMIC DATA

A Research Project Supported by a NASA Grant
in the Space Related Sciences

NsG-518

Project No. DRI-612

University of Denver

June 1966

SUBMITTED BY:

R. Gailor Justice

R. Gailor Justice
Principal Investigator
Chemical Engineering Department

N66-35770

ABSTRACT

The object of this work was to obtain some insight into the most efficient and sensitive procedure for data reduction and mathematical modeling of experimental process dynamic data. The physical system chosen for analysis was the dissipation of a tracer injection in a fluid flowing through a tube. The partial differential equation representing this system is the well known one-dimensional axial dispersion equation

$$\frac{\partial C}{\partial t} = D_L \frac{\partial^2 C}{\partial x^2} - \bar{u} \frac{\partial C}{\partial x}$$

The solutions of this equation in the time domain, the frequency domain and the Laplace domain are given in the body of the text. Thirty-three sets of experimental data with dynamic material balances varying from less than 1% to greater than 40% were analyzed. These data were correlated to the mathematical model in the three aforementioned domains. The Peclet number and the effective residence time were obtained by minimizing a residual surface using modified and steepest descent techniques. Normalized input, normalized output, and the raw data of all runs were processed in the time domain. Thirteen selected runs were processed in the frequency domain and only one run was processed in the Laplace domain. A consistent least squares argument between the time and frequency domain was developed and utilized. However, the transformation of this argument could not be made into the Laplace domain where real values for the Laplace variable are used.

In general it was found that no significant discrepancies existed between the parameters determined in the three domains. However, due to the behavior of the numerical Laplace transform around zero and the author's inability to transform a consistent least squares argument into this domain, it was decided to eliminate this method of data reduction from further consideration.

The Peclet number varied significantly between the normalized and unnormalized data when the material balance deviation was greater than approximately 15 percent. Normalization had little effect on the effective residence time.

Residual surfaces were found to be quite steep for variations in the effective residence time, whereas they were shallow and elongated for variations in the Peclet number.

The computation time was essentially the same for numerical convolution and numerical Fourier transform calculations. These programs were not optimized; however, the same logic form was utilized for both calculations when seeking parameters.

Author

TABLE OF CONTENTS

LIST OF FIGURES

LIST OF TABLES

INTRODUCTION

A. Pulse Testing:

One of the most useful techniques for obtaining experimental dynamics of linear systems is the pulse test. The pulse test is performed by forcing the system input with a pulse of finite duration and recording both the system input and its response.

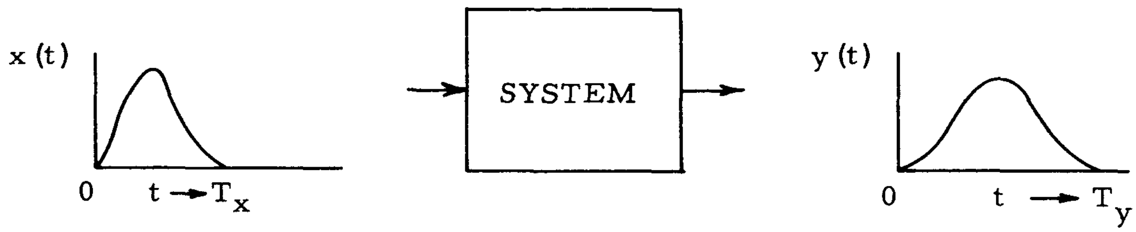

Figure 1. The Pulse Test

The resulting data can be modeled to a theoretical equation in either the time domain, the frequency domain, or the Laplace domain. The transfer function of the system is defined as

$$G(s) = \frac{y(s)}{x(s)} = \frac{\int_0^{T_y} y(t)\, e^{-st}\, dt}{\int_0^{T_x} x(t)\, e^{-st}\, dt} \tag{1}$$

Several authors[1,3] have used real values of s and numerical reductions of the experimental data according to Equation 1 to obtain the transfer function form. The experimental dynamics is then represented by a plot of G(s) versus s.

The Fourier transform can be applied to Equation 1 by substituting $j\omega$ for s, where j is the $\sqrt{-1}$. The resulting transform yields

$$G(j\omega) = \frac{\int_0^{T_y} y(t)\, e^{-j\omega t}\, dt}{\int_0^{T_x} x(t)\, e^{-j\omega t}\, dt} \tag{2}$$

Using the identity $e^{-j\omega t} = \cos\omega t - j \sin \omega t$, Equation 2 becomes

$$G(j\omega) = \frac{\int_0^{T_y} y(t)\cos\omega t \, dt - j\int_0^{T_y} y(t)\sin\omega t \, dt}{\int_0^{T_x} x(t)\cos\omega t \, dt - j\int_0^{T_x} x(t)\sin\omega t \, dt} \tag{3}$$

This is the system frequency response and it can be separated into its real and imaginary parts as

$$Re(\omega) = \frac{AC + BD}{C^2 + D^2} \tag{4}$$

$$Im(\omega) = \frac{AD - BC}{C^2 + D^2} \tag{5}$$

where

$$A = \int_0^{T_y} y(t) \cos \omega t \, dt \tag{6}$$

$$B = \int_0^{T_y} y(t) \sin\omega t \, dt \tag{7}$$

$$C = \int_0^{T_x} x(t) \cos \omega t \, dt \tag{8}$$

$$D = \int_0^{T_x} x(t) \sin\omega t \, dt \tag{9}$$

Numerical solutions of the above integrals yield the experimental dynamics in frequency response form. It can be represented by a Nyquist plot of $Re(\omega)$ versus $Im(\omega)$.

B. The Mathematical Model:

If the law of mass conservation is applied to a differential element of material flowing in a tube of length L at constant velocity, $\bar{u}$, the one dimensional axial dispersion equation is obtained as

$$\frac{\partial C}{\partial t} = D_L \frac{\partial^2 C}{\partial x^2} - \bar{u} \frac{\partial C}{\partial x} \tag{10}$$

where

C = concentration - mass/(length)^3

t = time

x = length

$\overline{u}$ = stream velocity, length/time

D_L = longitudinal dispersion coefficient, (length)^2/time.

Where the term $D_L\ \partial^2C/\partial x^2$ represents axial dispersion due to a concentration gradient and $u\ \partial C/\partial x$ represents the transportation of material due to bulk flow.

The initial and boundary conditions chosen for this study were

$$\begin{aligned} C(0, t) &= C_{in}(t) \\ C(L, t) &= C_{out}(t) \\ C(x, 0) &= 0 \\ \lim_{x \to \infty} C(x, t) &= 0 \end{aligned} \tag{11}$$

The infinite tube boundary condition was chosen rather than the boundary conditions given by Danckwerts[4]. This was done because the infinite tube boundary condition yields a closed form solution for the impulse response whereas the boundary conditions by Danckwerts yields an infinite series in exponentials. There is also very little difference in the frequency response when using this boundary condition.

The transfer function for Equation 10 can be obtained by Laplace transformation as

$$G(s) = \frac{C_{out}(s)}{C_{in}(s)} = \exp\left\{\frac{N_{Pe}}{2}\left[1 - \sqrt{1 + \frac{4\theta s}{N_{Pe}}}\right]\right\} \tag{12}$$

where

$\theta = L/\overline{u}$ = Residence time

$N_{Pe} = \dfrac{\overline{u}L}{D}$ = Peclet Number

For fixed values of the residence time and the Peclet number, the theoretical Laplace response, G(s), can be calculated from Equation 12 for real values of s, the Laplace variable. The experimental Laplace response can be correlated to the theoretical response by varying the residence time and the Peclet number.

The model frequency response is obtained from Equation 12 by substitution of $j\omega$ for s.

$$G(j\omega) = \exp\left\{\frac{N_{Pe}}{2}\left[1 - \sqrt{1 + j\,\frac{4\theta\omega}{N_{Pe}}}\right]\right\} \tag{13}$$

The real and imaginary portions of Equation 13 are

$$\begin{aligned} Re(\omega) = {} & \exp\left\{\frac{N_{Pe}}{2}\left[1 - \left(1 + \frac{4\omega\theta}{N_{Pe}}\right)^{\frac{1}{4}} \cos\left(\frac{1}{2}\tan^{-1}\frac{4\omega\theta}{N_{Pe}}\right)\right]\right. \\ & \times \cos\left\{-\frac{N_{Pe}}{2}\left(1 + \frac{4\omega\theta}{N_{Pe}}\right)^{\frac{1}{4}} \cos\left(\frac{1}{2}\tan^{-1}\frac{4\omega\theta}{N_{Pe}}\right)\right\} \end{aligned} \tag{14}$$

$$\begin{aligned} Im(\omega) = {} & \exp\left\{\frac{N_{Pe}}{2}\left[1 - \left(1 + \frac{4\omega\theta}{N_{Pe}}\right)^{\frac{1}{4}} \cos\left(\frac{1}{2}\tan^{-1}\frac{4\omega\theta}{N_{Pe}}\right)\right]\right\} \\ & \times \sin\left\{-\frac{N_{Pe}}{2}\left(1 + \frac{4\omega\theta}{N_{Pe}}\right)^{\frac{1}{4}} \cos\left(\frac{1}{2}\tan^{-1}\frac{4\omega\theta}{N_{Pe}}\right)\right\} \end{aligned} \tag{15}$$

The experimental frequency response can be correlated to the theoretical response by varying the residence time and the Peclet number.

The impulse response, the inverse Laplace transform of G(s) in Equation 12 is

$$G(t) = \sqrt{\frac{N_{Pe}\theta}{4\pi t^3}}\ \exp\left\{\frac{-N_{Pe}}{4t\theta}\,(t-\theta)^2\right\} \tag{16}$$

The time response of the system can be calculated using the convolution integral as

$$C_{out}(t) = \int_0^t C_{in}(\tau)\,G(t-\tau)\,d\tau \tag{17}$$

where τ is a dummy variable.

The experimental time response can also be correlated to the theoretical response by varying the residence time and Peclet number.

C. Least Squares Argument:

The least squares argument proposed for this work is given by

$$\underset{\text{(TIME DOMAIN)}}{\text{RESIDUAL}} = \Sigma\,[\underset{\text{MODEL}}{C_{out}(t)} - \underset{\text{EXPERIMENT}}{C_{out}(t)}]^2 \qquad (18)$$

This argument can be transformed into the frequency domain by use of Parseval's theorem[6] as

$$\underset{\text{(FREQUENCY DOMAIN)}}{\text{RESIDUAL}} = \Sigma\,(s\phi x(\omega))^2 \{[\underset{\text{MODEL}}{Re(\omega)} - \underset{\text{EXPERIMENT}}{Re(\omega)}]^2 + [\underset{\text{MODEL}}{Im(\omega)} - \underset{\text{EXPERIMENT}}{Im(\omega)}]^2\} \qquad (19)$$

where $(s\phi x)$ is the frequency content of the input pulse and is given by

$$s\phi x(\omega) = \sqrt{C^2 + D^2} \qquad (20)$$

where C and D are defined in Equations 8 and 9.

The author was unable to transform the least squares argument into the Laplace domain. There is also some doubt that this transformation actually exists since it is a nonlinear transformation. For this reason and because of the behavior of the numerical Laplace transform around zero this method was eliminated from further consideration.

D. Experimental Data and Normalization:

Thirty-three sets of axial dispersion data were utilized in this study. These data were from a Thesis by the author[5] and the procedure for their collection is described therein.

For the experimental system, mass must be conserved. Some of these data, however, did not agree with the dynamic material balance. That is, the area under the input pulse was not the same as the area under the response curve. Normalization factors were applied to both the input and output pulses in order to make the data obey the law of mass conservation. The normalization factor for the input data is given by

$$N = \frac{\int_0^{T_y} C_{out}(t)\, dt}{\int_0^{T_x} C_{in}(t)\, dt} \tag{21}$$

The normalization factor for the output data is the reciprocal of Equation 21.

E. Modified and Steepest Descent Correlation Techniques:

Modified and steepest descent correlation techniques as described by Marquardt[7] were utilized in this work. These techniques were developed for nonlinear correlations and are trial and error iteration procedures used to find the minimum of a residual surface.

The modified technique makes use of the rates of change of the residual with respect to the Peclet number and the residence time evaluated at a starting point for the trial and error search. A step proportional to the magnitude of the gradient and normal to the gradient was taken to a new point in terms of the parameters where the procedure was repeated. After several iterations a step size could be generated from previous knowledge of the shape of the residual surface.

The steepest descent technique minimizes the rates of change of the residual with respect to the step size. It generates both direction and step size.

The steepest descent technique generates large step sizes when the gradient is large. This causes the search to oscillate around the minimum or to step far to one side. Correction of the step size cannot be accomplished when using this procedure. Therefore all searches in this work were begun with the modified technique and switched to the steepest descent technique after the surface became less steep.

F. Objective and Procedure

The objective of this work was to gain some insight into the most efficient and sensitive procedure for reduction and mathematical modeling of process dynamic data.

This was accomplished by analyzing thirty-three sets of experimental data with dynamic material balances varying from less than 1% to greater than 40%. These data were reduced in the frequency domain using the numerical Fourier transform. The Laplace domain reduction was accomplished using the numerical Laplace transform with real and positive values of s, the Laplace variable. The time domain data and the reduced data were correlated to the mathematical model in the time domain, the frequency domain and the Laplace domain. These correlations were accomplished using modified and steepest descent techniques to minimize the residual in Equations 18 and 19.

A comparison between the parameters obtained in the above procedures was made in order to determine any discrepancies. A comparison was also made between the computation time required for the data reduction in the three domains to determine efficiencies.

These data were processed in the raw form and in the normalized form in all three domains. This gave a measure to the effect of data normalization.

COMPUTER PROGRAMS

Five computer programs were written for this study. These were:

1. Reduction of pulse test data to frequency response using the numerical Fourier transform. This was accomplished by modifying a program by Clements[3] which uses the quadrature formula of Filon. This formula is the most accurate available for the numerical evaluation of integrals of the type in Equations 6 through 9.

2. Reduction of pulse test data to Laplace response using the numerical Laplace transform. This was accomplished by modifying a program by Clements.[3] This procedure used a quadratic approximation of the experimental data and analytical integration over finite time divisions. Real values of s having the same values as the frequencies used in obtaining the numerical Fourier transform were utilized.

3. Modified and steepest descent program for correlation of frequency response data. This program utilized techniques described in section E of the introduction of this report. Included in this program were procedures to calculate the rates of change of the residual with respect to the two parameters. This required the calculation of the rates of change of the real and imaginary portions of the frequency response of the model with respect to the two parameters. Included also in this program was a procedure for plotting the Nyquist diagram of the correlation on the line printer. This allowed rapid visual interpretation of the degree of correlation.

4. Modified and steepest descent program for correlation of Laplace response data. The logic in the correlation program for the numerical Laplace transform data was the same as that used in the frequency response correlation. This correlation required the rates of change of the Laplace response of the model with respect to the two parameters.

5. A combination program for the calculation of the convolution integral and modified and steepest descent techniques for correlation of the time domain response. A flow diagram of this program is shown in Figure 2. The four main parts of this program are:

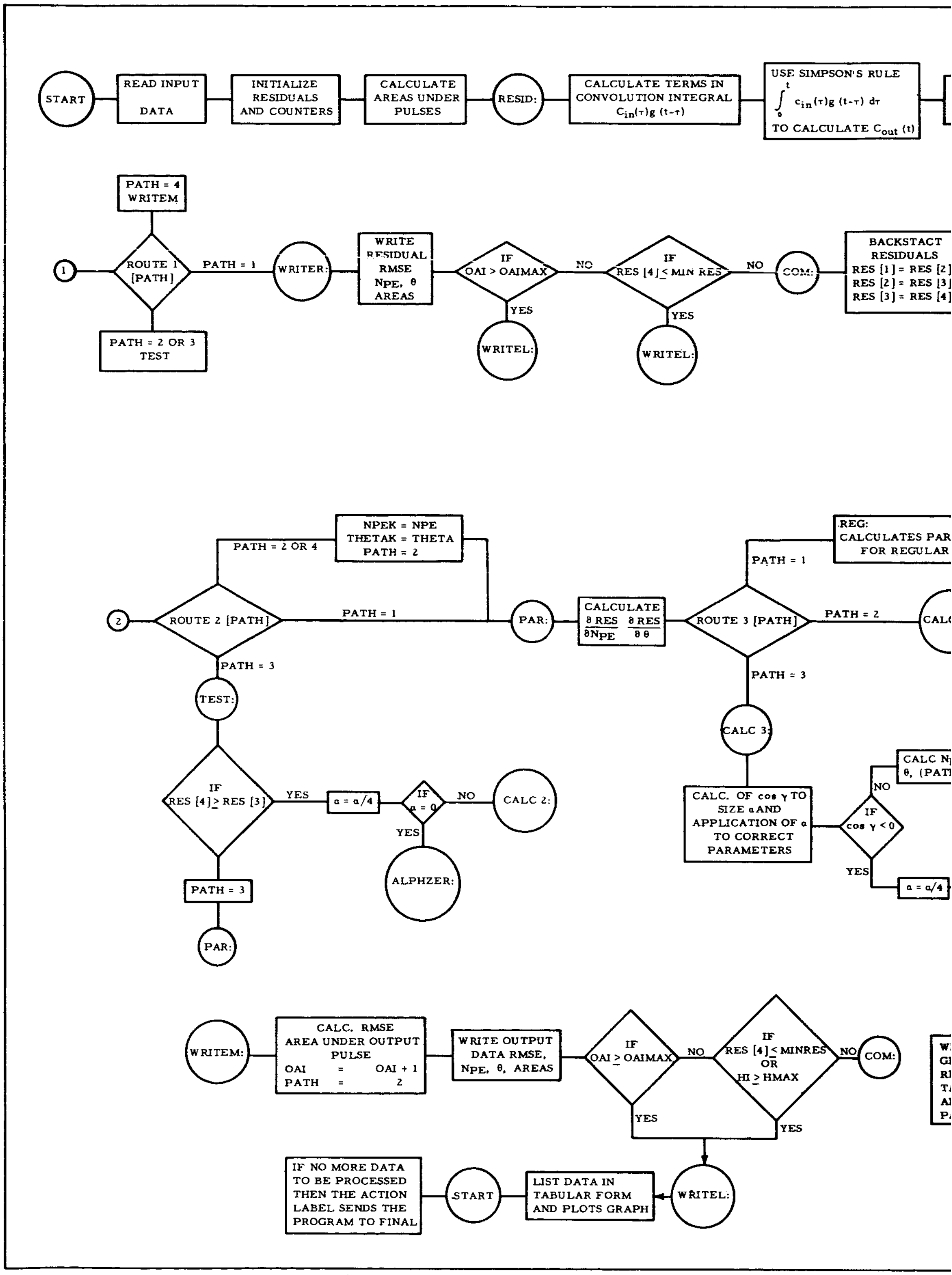

Figure 2. Flow Diagram of Time Dor

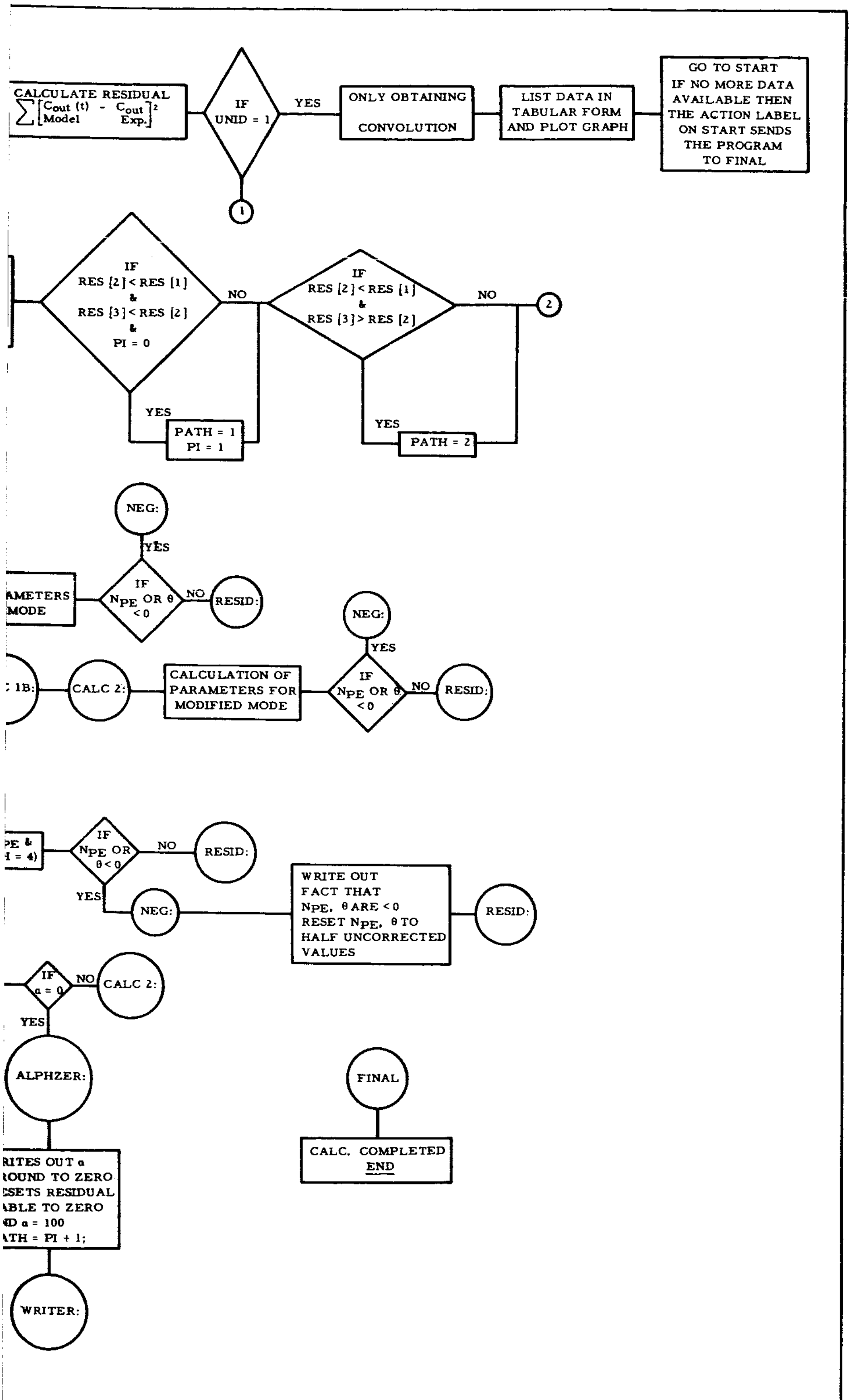

nain Correlation Program

2-2

a. The calculation of the convolution integral using the input forcing data, the impulse response and Simpson's one-third quadrature formula. The program will process pulse data that has been subdivided using two separate panel widths.

b. The calculation of the rates of change of the residual with respect to the two parameters. This also requires the use of the convolution integral and Simpson's one-third rule.

c. Generation of the directions for changes of the parameters in the modified mode. This portion of the program utilizes a step size which is refined as knowledge about the residual surface is gained. The modified mode is used in the first two optimum seeking steps and also at the bottom of the residual surface where steepest descent techniques tend to oscillate. This part of the program used the information calculated in step (b) above.

d. Generation of both step and direction for the parameters in the steepest descent mode. This portion of the program utilizes the rates of change of the residual with respect to the two parameters as calculated in step (b) above.

RESULTS AND CONCLUSIONS

Figures 3 and 4 show a typical correlation of an experimental run. Figure 3 shows the time domain correlations for both normalized and unnormalized data. The material balance deviation for Run D-39 was 18%. The normalized correlation is almost perfect whereas the unnormalized correlation must adjust for the material balance deviation. The residence time is essentially the same for both the normalized and unnormalized data. There is, however, a 75% deviation between the Peclet numbers in the two cases, 208.7 compared to 139.5. There is a two-fold standard deviation difference between the correlations, 1.73×10^{-3} compared to 3.95×10^{-3}. An attempt to compare these two values using an F ratio test[2] was made. It was found that there was a definite statistical difference between these two sets of data even at 99.5% confidence limits.

It was hoped that in the beginning of these studies that statistics could be used to make a decision on which data to discard because of material balance deviation. Using F ratio tests, it was found that all data having a material balance deviation greater than 5% would have to be discarded to maintain 95% confidence limits. This would have meant that all but six of the 33 runs would have to be discarded. Data of this type is extremely difficult to obtain, especially when some pulses remain in the packed tube for more than five minutes. The material balance error seemed to be random. In some cases more material was detected in the outlet than in the inlet and in some cases the opposite was found. Due to the random nature of the material balance error, no runs were discarded.

Figure 4 shows the same correlation in the frequency domain. Again an almost perfect fit was obtained in the normalized correlation.

Figure 5 shows the residual surface for the time domain correlation of D-37. Five search steps were needed to locate the optimum of the surface. The first two steps were made in the modified mode. These steps were taken normal to the gradient of the surface. The last three steps were made in the steepest descent mode.

The residual surface is very steep for changes in the residence time whereas it is shallow for changes in the Peclet number. The residence time centers the pulse on the time axis and the Peclet number determines the height of the pulse. These surfaces tend to point out the need for very accurate determinations of the residence time in the

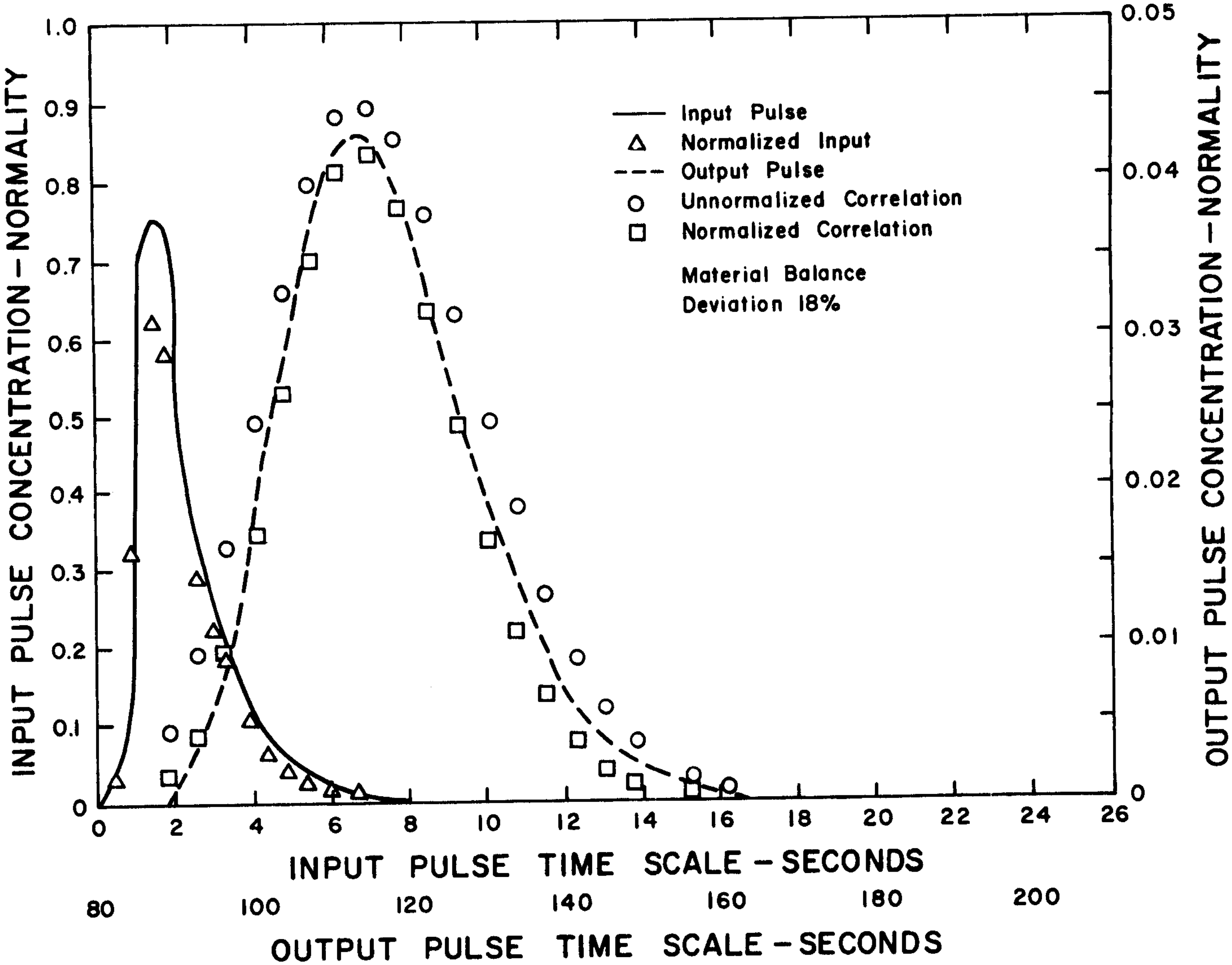

Figure 3. Time Domain Correlation of D-39

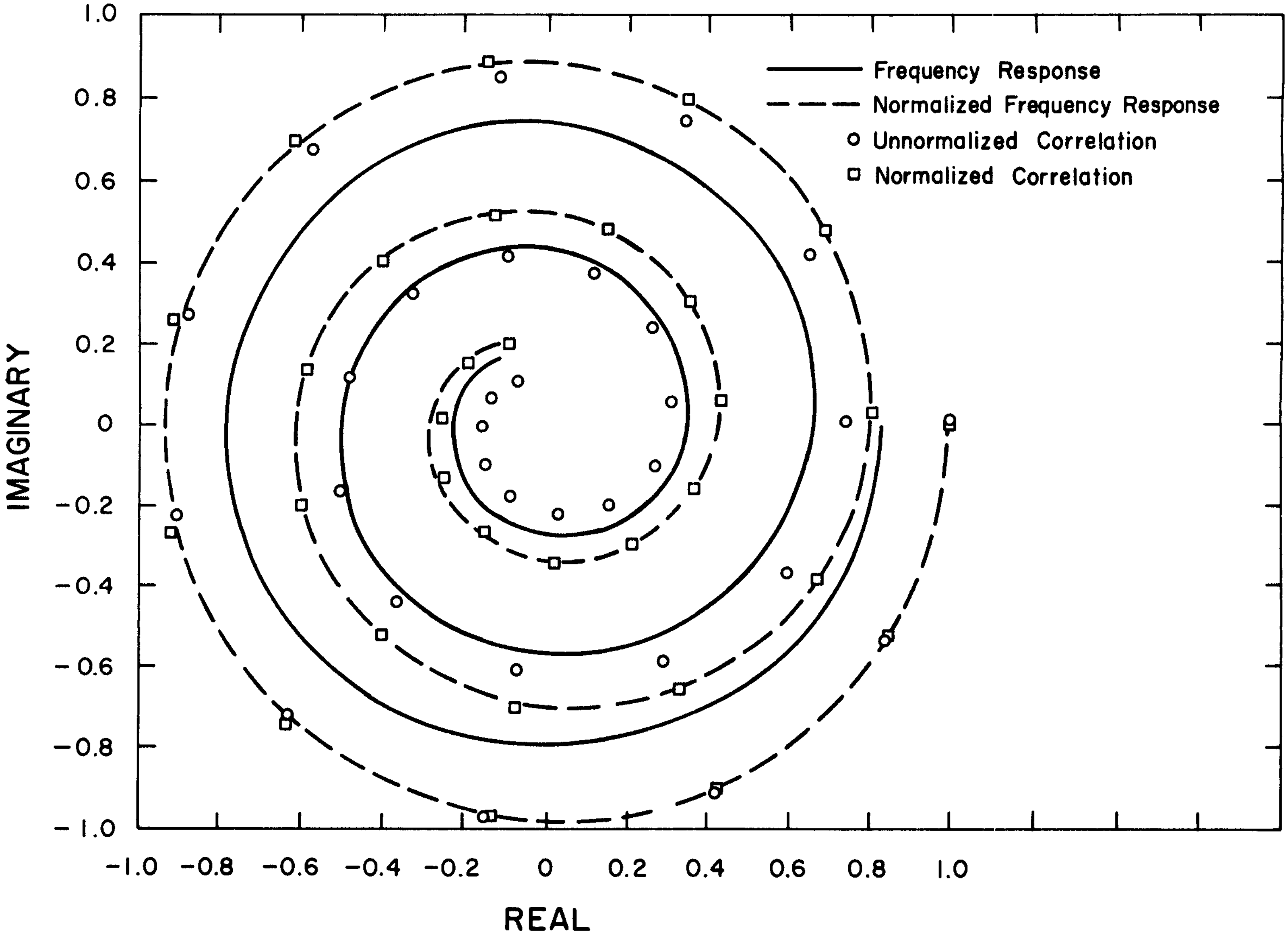

Figure 4. Frequency Domain Correlation of D-39

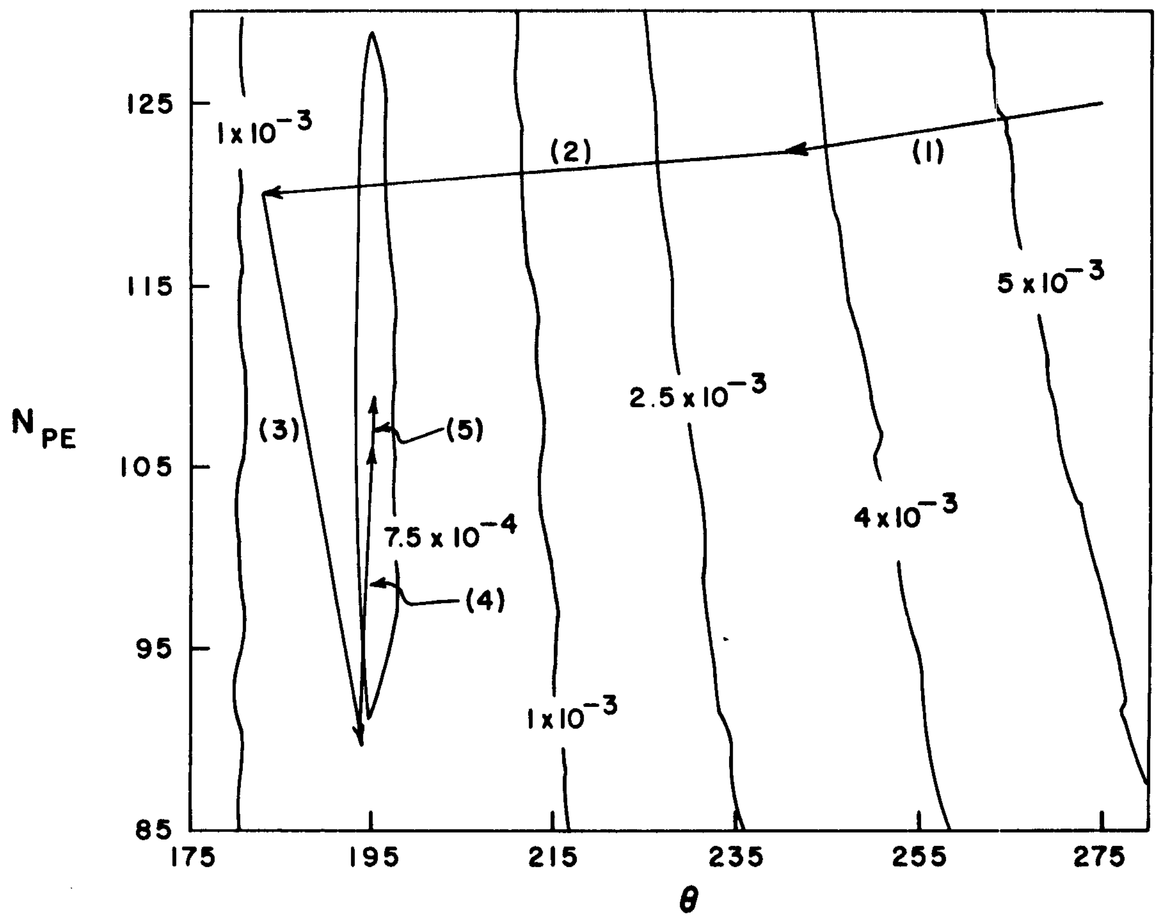

Figure 5. Time Domain Residual Surface of D-37

tube. It can be seen in Table 1 that the residence time for the normalized and unnormalized data is essentially the same no matter which domain is chosen for data reduction.

Figure 6 shows the residual surface determined in the frequency domain correlation. Four search steps were required to obtain the optimum. The first two were by the modified mode whereas the last two were in the steepest mode. In general four or five steps from an initial guess were required to reach the optimum in all runs.

Table 1 is a listing of the parameters obtained in selected runs. There is very little difference in residence times obtained from normalized or unnormalized data or from processing the data in the time or the frequency domain. There is very little difference between the parameters obtained in time domain modeling and those obtained in frequency domain modeling. There is a difference between the Peclet numbers determined from the normalized and those determined from the unnormalized data. The difference, however, becomes prominent only when the material balance deviation is greater than 15%. Even at that point there is very little difference in the time domain responses as the residual surface is not very sensitive to changes in the Peclet number.

Figure 7 is a plot of the Peclet numbers as a function of a characteristic Reynolds number. The Peclet number seems to be constant with increasing Reynolds number at a value of approximately 0.6. This is in agreement with Strange and Geankoplis[8] who obtained essentially the same result using sinusoidal testing techniques.

One correlation was processed using the numerical Laplace transform. This correlation was on the unnormalized data of D-31. The same numerical values used for frequency in the data reduction to frequency response were used for the Laplace variable. The Peclet number obtained was 33.6 compared to 48.4 for the time domain modeling and 59.3 for the frequency domain modeling. The residence time obtained was 982 compared to 702 for the time domain modeling and 673 for the frequency domain modeling. An investigation was conducted into the behavior of the numerical Laplace transform to try and determine the reason for this discrepancy. It was discovered that the numerical Laplace transform gave the area under the pulse at s equal to zero and for small values of s it dropped off quite rapidly to a very small number. The ratio of two such small numbers to give G(s) causes significant error. As s increases the numbers become progressively larger and

Table 1. Comparison of Parameters Obtained in Modeling Studies

Run Number	Material Balance Deviation	Normalized Data						Unnormalized Data					
		Time Domain			Frequency Domain			Time Domain			Frequency Domain		
		N_{Pe}	θ	$\sigma \times 10^4$	N_{Pe}	θ	$\sigma \times 10^2$	N_{Pe}	θ	$\sigma \times 10^4$	N_{Pe}	θ	$\sigma \times 10^2$
D-31	38%	140.1	659	7.0	132.6	654	5.10	48.4	702	46.9	59.3	673	49.5
D-32	40%	143.8	843	6.9	135.7	830	6.7	42.0	876	67.9	56.3	856	73.2
D-33	8%	135.9	1389	6.9	113.6	1335	13.8	113.5	1397	15.0	96.0	1341	24.9
D-34	22%	134.0	2283	5.3	122.4	2230	8.2	87.3	2309	28.3	77.0	2258	59.4
D-35	25%	151.1	90	12.3	146.9	89	3.5	90.1	92	44.8	92.9	91	13.8
D-37	1%	108.8	195	14.1	100.7	194	8.2	107.1	195	14.9	99.3	194	8.5
D-38	46%	191.6	287	8.1	195.9	285	1.7	29.7	306	63.4	63.9	293	40.1
D-39	18%	208.7	115	17.3	181.6	114	2.3	139.5	116	39.5	131.0	115	12.7
D-49	21%	94.6	433	8.9	81.9	415	5.3	62.9	439	43.5	54.5	422	33.1
D-50	7%	76.3	158	27.4	67.9	155	12.0	85.7	157	18.4	77.2	154	10.9
D-52	3%	66.9	451	24.6	58.5	434	16.8	70.9	450	24.3	61.9	432	17.0
D-59	27%	45.1	74	27.1	38.7	70	2.6	25.9	78	103.0	21.7	74	27.9
D-61	35%	41.3	94	24.2	37.9	91	3.1	19.3	102	119.1	18.2	98	36.9

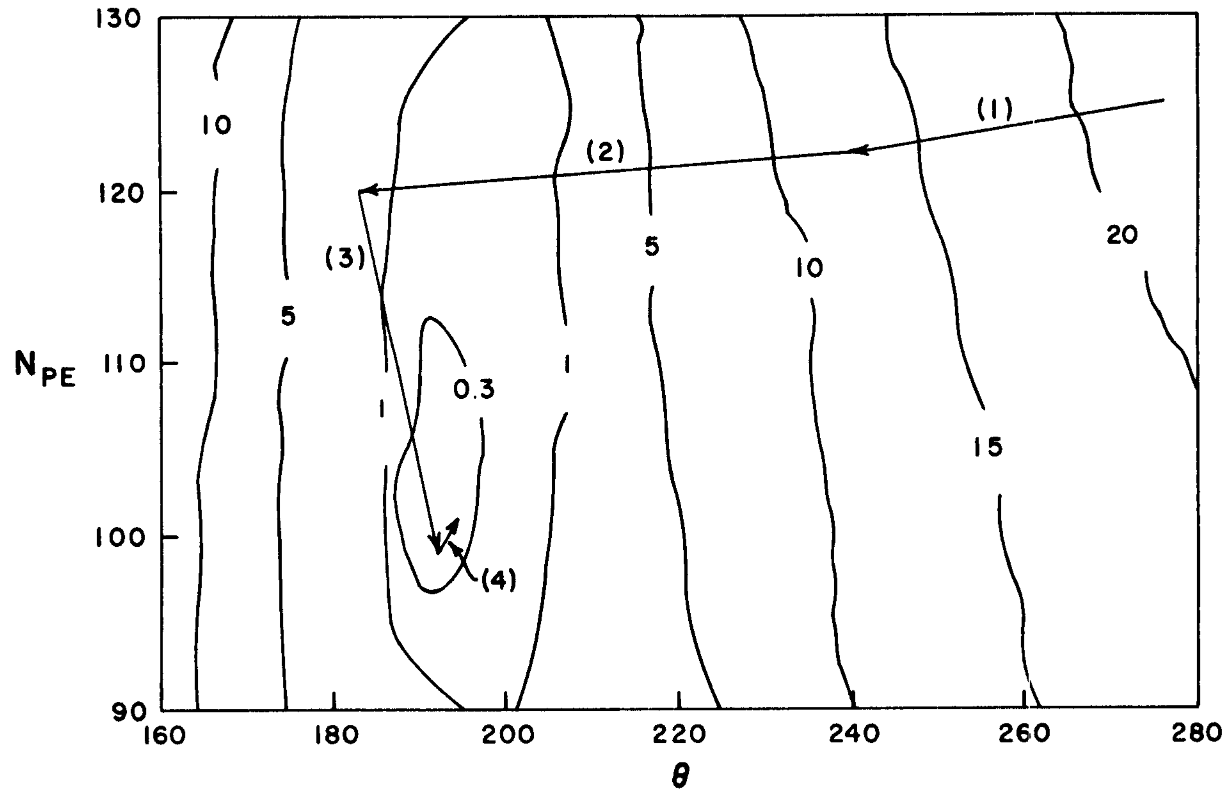

Figure 6. Frequency Domain Residual Surface of D-37

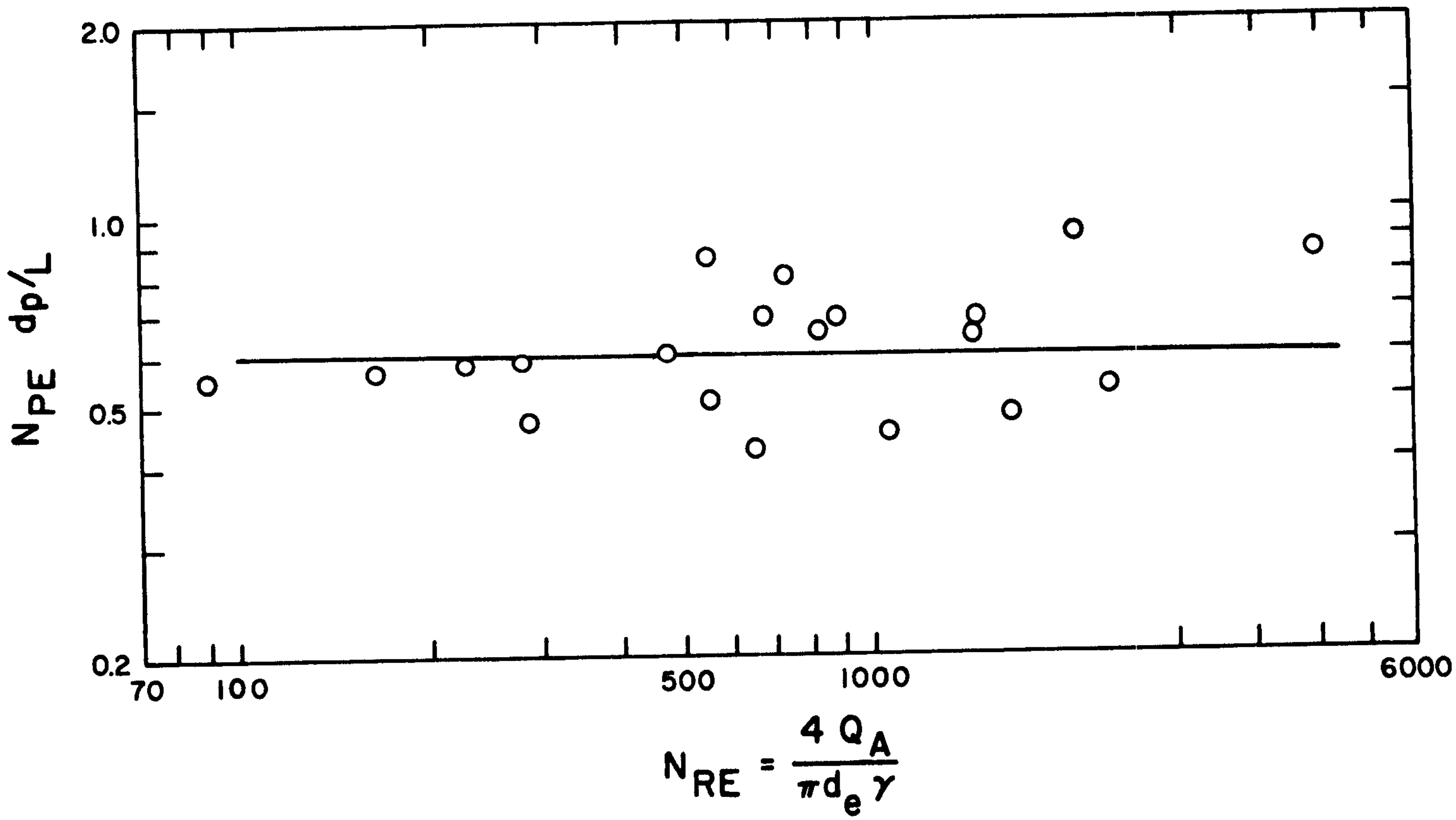

Figure 7. Characteristic Reynolds Number versus Peclet Number

the errors seem to disappear. As was stated previously, the author was unable to transform a consistent least squares argument into the Laplace domain. Due to this and to the behavior of the numerical Laplace transform around zero this method of data reduction was given no further consideration.

Time studies were made to determine computer processing time for modeling in the frequency and time domains. Each iteration in the frequency domain required approximately eight seconds and the frequency response calculation required approximately three seconds. Each iteration in the time domain required approximately ten seconds. Extensive studies were not made; however, the runs that were timed generally converged to the optimum in less than 40 seconds. No significant difference in processing time between the two domains was observed.

TABLE OF NOMENCLATURE

A, B, C, D	-	Intermediate Variables Defined in Text.
$C(t)$	-	Concentration, M/L^3.
d_e	-	Equivalent Tube Diameter, L.
d_p	-	Packing Particle Diameter, L.
D_L	-	Axial Dispersion Coefficient, L^2/T.
$G(s)$	-	System Transfer Function.
$G(t)$	-	Impulse Response.
$Im(\omega)$	-	Imaginary Portion of Frequency Response.
j	-	$\sqrt{-1}$.
L	-	Column Length, L.
N	-	Normalization Factor.
N_{Pe}	-	Peclet Number.
N_{Re}	-	Reynolds Number.
Q_A	-	Flow Rate, L^3/T.
$Re(\omega)$	-	Real Portion of Frequency Response.
s	-	Laplace Variable.
$s\phi x$	-	Input Pulse Frequency Content.
t	-	Time, T.
T_x	-	Input Pulse Width, T.
T_y	-	Output Pulse Width, T.
$\overline{u}$	-	Stream Velocity, L/T.
x	-	Length Ordinate, L.
$x(t)$	-	Input Pulse Abscissa.
$y(t)$	-	Output Pulse Abscissa.

Greek

θ	-	Residence Time, T.
ω	-	Frequency, 1/T.
γ	-	Kinematic Viscosity, L^2/T.
τ	-	Dummy Variable

LIST OF REFERENCES

1. Adler, R. J., "Finite Stage Modeling," Paper presented at the Fourth National I. S. A. Chemical and Petroleum Instrumentation Symposium, Wilmington, Delaware, April, 1962.

2. Bennett, C. A., "Statistical Analysis in Chemistry and the Chemical Industry," John Wiley and Sons, Inc., New York, 1954.

3. Clements, W. C., Jr., "Pulse Testing for Dynamic Analysis," Ph.D. Thesis, Vanderbilt University, 1963.

4. Danckwerts, P. V., Chem. Eng. Sci. 2, 1 (1953).

5. Justice, R. G., "Frequency Response of Single Phase Longitudinal Dispersion and Two-Phase Extraction in Packed Beds Using Pulse Testing Methods," Ph.D. Thesis, Vanderbilt University, 1963.

6. LePage, W. R., "Complex Variables and the Laplace Transform for Engineers," McGraw-Hill Book Co., New York, 1961.

7. Marquardt, D. W. Chem. Eng. Prog. 55, 65 (1959).

8. Strange, D. A. and Geankoplis, C. J., Ind. Eng. Chem. 50, No. 9, 1305 (1958).